The Astrophysical Journal, 699:1389–1394, 2009 July 10 doi:10.1088/0004-637X/699/2/1389

INTERNAL DYNAMICS AND DYNAMICAL FRICTION EFFECTS IN THE DWARF SPHEROIDAL GALAXY IN FORNAX

Ramanath Cowsik[1], Kasey Wagoner[1], Emanuele Berti[2,3], and Amit Sircar[1]
[1] McDonnell Center for the Space Sciences, Department of Physics, Washington University, St. Louis, MO 63130, USA
[2] Department of Physics and Astronomy, The University of Mississippi, University, MS 38677-1848, USA
[3] Jet Propulsion Laboratory, California Institute of Technology, Pasadena, CA 91109, USA
Received 2008 December 16; accepted 2009 April 29; published 2009 June 23

ABSTRACT

In the Fornax dwarf spheroidal galaxy the globular clusters are distributed widely, without any significant central concentration. Oh et al. pointed out that such a distribution is paradoxical: dynamical friction effects estimated using single-component King models would have forced the globular clusters to spiral down to the center of the galaxy well within a Hubble time. This paper is devoted to a discussion of this paradox. We describe a model in which the stars of the dwarf spheroidal galaxy are embedded in a cloud of dark matter, and each of these components is specified by its own phase-space distribution function. This model allows us to fit self-consistently the observed luminosity profile and the spatial variation of the velocity dispersion of the stars. This fitting yields two basic parameters, related to the central density and velocity dispersion, that characterize the phase-space distribution of dark matter. The dynamical friction effects calculated on the basis of this self-consistent model are small enough that the observed spatial distribution of the globular clusters poses no difficulty, and the apparent paradox is resolved. Thus, we have at hand a model for Fornax that reproduces the main observed features of this dwarf spheroidal galaxy.

Key words: dark matter – galaxies: dwarf – galaxies: kinematics and dynamics

1. INTRODUCTION

The masses and the phase-space structure of the smallest stellar systems that form in the universe provide the most direct clues to decipher the nature of dark matter and the process of galaxy formation. Among these systems, dwarf spheroidal galaxies are the most suitable for the study of dark matter. They have low densities of visible matter in the form of stars (about a million times smaller than those encountered in globular clusters of comparable masses), and both their internal and external dynamics are dominated by the cloud of dark matter (more commonly called the halo) in which they are embedded. Their stability against tidal disruption and also their internal dynamics depend upon details of the structure and extent of the dark matter cloud, which in turn is sensitive to the phase-space structure of the dark matter particles constituting the halo.

In recent years, improved astronomical observations of these faint systems have become available for comparison with theoretical studies. One of the earliest studies of these systems is by Faber & Lin (1983), who used luminosity profile observations to show that dwarf galaxies are dominated by dark matter even in their cores, drawing attention to dwarf spheroidal galaxies as candidates for the study of dark matter. Around the same time, Aaronson (1983) measured the radial velocities for several carbon stars in these systems with sufficient accuracy to support the idea that dark matter plays a dominant role in their internal kinematics. Prompted by these studies, Cowsik & Ghosh (1986, 1987) developed an "embedding model" where the dwarf spheroidals are embedded in an extensive cloud of dark matter. A similar approach was championed by Pryor & Kormendy (1990) in the context of dwarf spheroidal galaxies. Tremaine (1976) and Hernandez & Gilmore (1998) discussed dynamical friction effects on globular clusters in dwarf galaxies. They derived simplified analytical formulas for the orbital evolution of a massive body in a dark halo which is assumed to follow the King distribution (King 1966; Binney & Tremaine 2008), finding that the dynamical timescales for the globular clusters to sink to the center of the galaxy are about 1 Gyr, and that these timescales increase as the core radius increases.

Of particular relevance to the present study is the work of Oh et al. (2000), who pointed out that the five globular clusters gravitationally bound to the dwarf spheroidal galaxy in Fornax paradoxically "preserve their diffuse spatial distribution despite the fact that the clusters' orbital decay timescale is much shorter than the estimated age of the host galaxy." Ciotti & Binney (2004) and Sanchez-Salcedo et al. (2006) have shown that the problem is exacerbated if modified Newtonian dynamics is applicable. There is a similar problem with the orbital decay timescales in dwarf elliptical galaxies (for details see e.g., Lotz et al. 2001). Goerdt et al. (2006) considered the effects of dynamical friction in dark matter halos with profiles having a central cusp, as suggested by cosmological simulations (Hernquist 1990; Navarro et al. 1997; Moore et al. 1999) and showed that "in a cuspy cold dark matter (CDM) halo the globulars would sink to the center from their current position within a few Gyr, presenting a puzzle." They further point out that should the stellar population be embedded in a dark matter halo with a large core, this difficulty would be resolved. In making this point, Goerdt et al. (2006) assume that the dark matter halo has a density profile given by

$$\rho(r) = \rho_D(0)[1 + (r/r_s)]^{-3}, \quad (1)$$

with a central density $\rho_D(0) = 0.1\ M_\odot\ \mathrm{pc}^{-3}$ and the scale size $r_s = 2.4$ kpc. They also assume that the density sharply cuts off at ∼50 kpc. Thereafter Jeans' equations representing the balance between gravitational forces, and the gradient in pressure provides them with the $\langle v^2(r)\rangle$ for this assumed density profile. This allows them to estimate the timescales for the dynamical friction to operate and conclude that in such a halo the dynamical friction effects on the globular clusters are small. This immediately opens up the following questions.

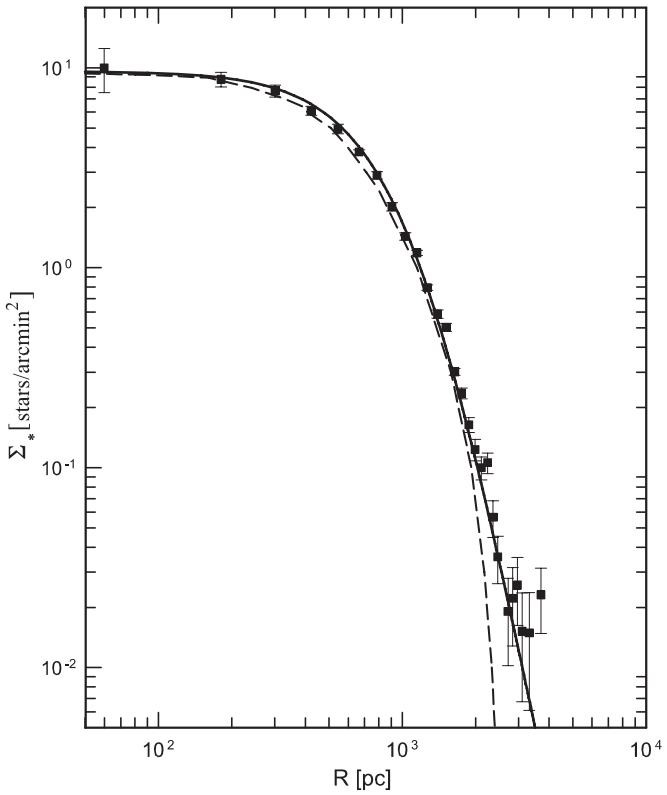

Figure 1. Theoretically calculated surface density in Equation (8) (solid black line) is compared with the observations by Coleman et al. (2005) and their single-component King model fit (dashed line corresponding to $\sigma_* \approx 11$ km s^{-1} and $r_{k*} \approx 2.6$ kpc), which progressively falls below the observed surface densities at distances beyond the core radius. The embedding model (solid black line) provides a very good fit.

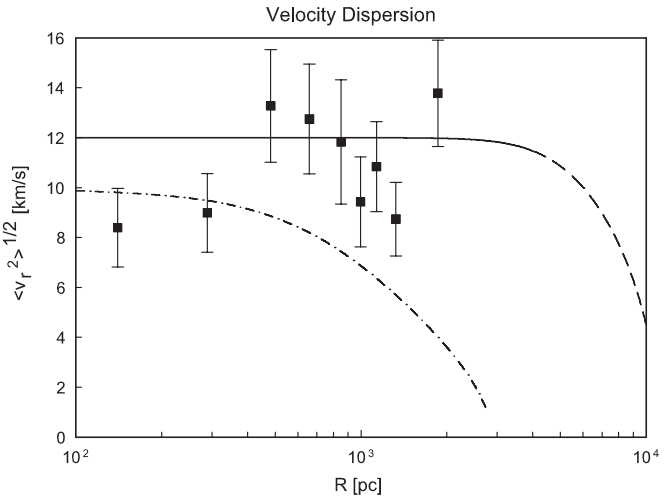

Figure 2. Observed dispersion in the radial velocities using 182 stars (Walker et al. 2006) is compared with our theoretical model (solid black line). A single-component King model presented by Walker et al. (dash-dot line) with $\phi(0)/\sigma_*^2 = 3.26$ and tidal radius $r_{k*} \approx 3$ kpc predicts smaller dispersion velocities beyond the core radius.

(1) Does the density distribution for dark matter given in Equation (1), with the chosen values for the parameters $\rho_D(0)$ and r_s, represent correctly the density profile of the dark matter halo in Fornax? (2) Would the stars embedded in such a halo follow the observed spatial distribution? (3) Would the observed $v_{*\mathrm{rms}}(r)$ of these stars be correctly reproduced?

In other words, in order to explicitly resolve the problem posed by the wide distribution of globular clusters in Fornax, we should work within the context of a model that will allow us to formally derive the density profile $\rho_*(r)$ of the stars and the profile of their velocity dispersion $v_{*\mathrm{rms}}(r)$ in terms of the parameters describing the phase-space distribution of dark matter. Such a phase-space distribution, with the best choice for the parameters, may then be inserted into the relevant integral in Chandrasekhar's formula to estimate the time constant for the migration of globular clusters toward the center of Fornax. As a follow-up of the earlier work of Tremaine (1976), Hernandez & Gilmore (1998), and Goerdt et al. (2006), this paper describes an attempt to construct such a model and address the problem posed by the wide distribution of globular clusters in Fornax.

Fortunately, aiding the model building effort, astronomical observations of the dwarf spheroidal galaxy in Fornax have improved considerably since the pioneering studies by Hodge (1961a, 1961b), and now excellent data sets are available. The galaxy is located at a distance of ∼138 kpc (Mateo 1998). It covers a large area of the sky, with an estimated tidal radius of ∼71′ (Irwin & Hatzidimitriou 1995), corresponding to ∼2.85 kpc. A careful wide-field survey by Coleman et al. (2005) provided a precise radial number density profile of the RGB-selected stars, showing that the observed distribution increasingly deviates from a single-component King distribution beyond the core radius (see Figure 1). The surface density beyond the core radius falls off as a power law and significant densities were noted up to 90′, far beyond the earlier estimates of the tidal radius. Walker et al. (2006) measured the radial velocities of a large number of stars in the galaxy and derived the radial velocity dispersion $\left\langle v_r^2(R)\right\rangle^{1/2}$ as a function of the projected distance R. They noted that the radial dependence is flat, again deviating significantly from the decreasing behavior as a function of R that would be expected for a single-component King distribution (Figure 2). The five globular clusters that pose a problem for dynamical friction timescales are located at projected distances $R = 0.24, 0.43, 1.05, 1.43$, and 1.60 kpc, respectively (Walker et al. 2006). Of course, their actual radial distances would be larger by a factor of $\sim \sqrt{3/2}$ on the average.

In order to model the observations noted above, we derive in Section 2 the radial dependence of the velocity dispersion and the surface density profile of stars within the context of a dynamical model by formulating the Boltzmann–Poisson equations in the embedding approximation. The solution to these equations is obtained through a standard procedure, which is briefly described. We assume that the underlying phase-space distributions, both for the dark matter and for the stars, are nearly isothermal and follow the lowered isothermal distributions (King 1966). In making this choice, we were guided by extensive earlier work adopting lowered isothermal phase-space distributions to model these systems (see for example Irwin & Hatzidimitriou 1995; Binney & Tremaine 2008 and references therein), as well as by the requirement of simplicity. Since there are two components in the Fornax system—the dark matter particles and the stars—we need at least two distributions to specify them, and the reduced isothermal distributions have the advantage that they form cored systems with finite masses and have been adopted extensively before for modeling various astronomical systems, including the dwarf spheroidal galaxies. It is perhaps relevant to point out here that recently some concerns have been expressed regarding their applicability to galactic systems (Gilmore et al. 2007). These authors have noted that the two-body relaxation time in these systems, $\tau_2 \approx (8N/\log N)\tau_{\mathrm{cross}}$, is much longer than the age of the universe, and as such the system would not have relaxed

to a nearly Maxwellian phase-space distribution. This remark is true and the absence of any segregation of massive stars into the central regions (except in the case of the densest globular clusters) indeed points to the absence of such equilibrium induced by two-body interactions. However, the smooth density profiles of these systems and our ability to model them with reduced isothermal distribution functions beg for an explanation. The pioneering study by Lynden-Bell (1967) has shown that the equilibria in such systems are dictated by collective effects. He showed that even though the "fine-grained" distribution takes almost infinite time to evolve, the "coarse-grained" distribution function rapidly relaxes due to collective effects into a quasi-stationary state—a process called "violent relaxation". His work triggered wide-ranging studies of the collective effects of long-range forces. As long as initial conditions avoid parametric oscillations and kinetic energy approximately balances the potential energy, $2T + U \approx 0$, the coarse-grained distribution does turn out to be quasi-Maxwellian (Levin et al. 2008). It may be noted further that it is the fluctuation of the gravitational potential due to collective effects that brings about this quasi-stationary state: all stars acquire the same distribution of velocities and there is no segregation, in contrast to equilibria driven by two-body interactions. Accordingly, we adopt reduced isothermal distribution functions for the stars and dark matter particles, solve self-consistently the equations of the embedding model, and therefrom compute the slowdown rate due to dynamical friction. In Section 3, we compare the theoretical predictions with the observed velocity dispersion and luminosity profile, and we show that the model indeed fits the observations very well. Thus, the main parameters of our model (a density parameter ρ_{CD} and a velocity dispersion parameter σ_D) are determined with sufficient accuracy, allowing us to estimate with confidence the time needed for the globular clusters to sink to the center due to dynamical friction. This turns out to be longer than the Hubble time, thereby resolving the paradox. Section 4 is devoted to a general discussion and concluding remarks.

2. THE DYNAMICAL MODEL

We begin the theoretical analysis by developing a dynamical model for the dwarf galaxy in Fornax. A comparison of the predictions of the model with the observations of the profiles of the rms of the line-of-sight velocities $v_{\rm rms*}(R)$, and the projected number density, $\Sigma_*(R)$, of the stars shows that the model provides an excellent fit to the observations and provides the best values of the two basic parameters ρ_{CD} and σ_D characterizing the phase-space distribution function of the dark matter particles in Fornax. Using these, we analytically integrate the incomplete integral over the phase-space distribution appearing in the Chandrasekhar formula for dynamical friction.

Let the phase-space distribution both of the dark matter f_D and the stars f_* be of the "reduced isothermal" form (King 1966)

$$\begin{aligned} f_i &= \rho_{Ci}(2\pi\sigma_i^2)^{-3/2}[e^{\varepsilon_i/\sigma_i^2} - 1] \text{ for } \varepsilon_i > 0\,, \\ &= 0 \text{ for } \varepsilon_i \leqslant 0\,. \end{aligned} \tag{2}$$

The subscript i could either be "D" or "$*$" for the particles of dark matter or the stars as appropriate, and the "binding energy" ε is given by

$$\varepsilon_i = \{\phi(r_{Ki}) - \phi(r) - v^2/2\} \equiv \{\xi_i - v^2/2\}\,, \tag{3}$$

where $\phi(r) = \phi_D(r) + \phi_*(r)$ is the total gravitational potential deriving contributions from dark matter and the stars. The terminal radii r_{Ki} for the two components are indirectly specified by the choice of the value of the total potential ϕ at these locations. Since the total gravitational potential due both to the dark matter and the stars occurs in both the distribution functions, it couples the two components. Note that these distribution functions depend only on v_2 which implies isotropy for the velocity distribution, and the distribution functions, being functions of energy alone, satisfy the stationary collisionless Boltzmann equation. The parameter r_{Ki} represents the apogalacticon at which the density vanishes, and this is indirectly specified by the choice of $[\phi(r_{Ki}) - \phi(0)]$. The integral over the velocities (King 1966; Binney & Tremaine 2008) provides the spatial density $\rho_D(r)$ and $\rho_*(r)$:

$$\rho_i = \rho_{Ci}\left[e^{y_i}\,\mathrm{erf}\left(y_i^{1/2}\right) - \sqrt{\frac{4y_i}{\pi}}\left(1 + \frac{2}{3}y_i\right)\right], \tag{4}$$

where $y_i = \xi_i/\sigma_i^2$ are the scaled potentials satisfying the spherically symmetric Poisson equations

$$\frac{2}{r}\frac{dy_i}{dr} + \frac{d^2y_i}{dr^2} = -\frac{4\pi G}{\sigma_i^2}\rho_i(r)\,. \tag{5}$$

Note that both $\rho_D(r)$ and $\rho_*(r)$ are functions of the total potential $\phi(r) = \phi_D(r) + \phi_*(r)$. This represents the coupling between the two systems; as the density of one of these becomes higher its contribution increases and the total potential becomes deeper, making both components more compact. Accordingly, these equations represent two coupled nonlinear differential equations, which are solved by the Taylor expansion of y_i about the origin, say up to the sixth order in r, and thence integrated using standard numerical methods (an adaptive Runge–Kutta scheme) to extend the solutions from small values of r to any desired distance. Noting that the mass-to-light ratio of dwarf spheroidals, including that in Fornax, are very large, we are able to simplify the numerical analysis by neglecting the contribution of the stars to the overall gravitational potential $\phi(r)$. From the numerical values of y_D and dy_D/dr, all quantities of interest may be evaluated: for example, the circular velocity $v_c(r) = \left\{\sigma_D^2 r|dy_D/dr|\right\}^{1/2}$, and the mass of dark matter contained within a radius $M_D(r) = \sigma_D^2 r^2|dy_D/dr|/G$. Furthermore, noting that with dominance of dark matter

$$y_*(r) = [y_D(r) - y_D(r_{K*})]\,\sigma_D^2/\sigma_*^2\,, \tag{6}$$

the density of the stars is evaluated using Equation (4). Now, the projection of any variable $Z(r)$ on the plane of the sky is given by

$$S(Z, R) = \int_R^{r_{\rm max}} 2Z(r)\frac{r\,dr}{(r^2 - R^2)^{1/2}}\,, \tag{7}$$

where R is the projected radial distance. With this, the surface density profile of stars is given by

$$\Sigma_*(R) = S(\rho_*(r), R)\,. \tag{8}$$

Defining the second moment of the phase-space distribution of stars as

$$\begin{aligned} T_*(r) &= \int_0^{\sqrt{2\xi_*}} f_* v^2 \cdot 4\pi v^2 dv \\ &= 3\rho_{C*}\sigma_*^2\left[e^{y_*}\,\mathrm{erf}(y_*^{1/2}) - \frac{8}{3\sqrt{\pi}}\left\{\frac{y_*^{5/2}}{5} + \frac{1}{2}y_*^{3/2} + \frac{3}{4}y_*^{1/2}\right\}\right] \end{aligned} \tag{9}$$

and recalling the assumption of isotropy,

$$\langle v_*^2(r)\rangle = \frac{T_*(r)}{3\rho_*(r)} \text{ and } v_{rms,*}(R) = \left[\frac{1}{3}\frac{S(T_*,R)}{S(\rho_*,R)}\right]^{1/2}. \quad (10)$$

In Equations (7)–(10), we have the theoretical functional forms for the profile of stellar surface density $\Sigma_*(R)$ and the profile of stellar velocity dispersion $v_{\rm rms*}(R)$, which may be compared with the corresponding profiles obtained from observations to determine the best choice of the parameters entering the distribution functions.

Now, Chandrasekhar's formula (Chandrasekhar 1943; Binney & Tremaine 2008) provides an estimate of the dynamical friction acting on the globular clusters in Fornax:

$$\frac{d\vec{V}}{dt} = -\frac{\vec{V}}{|V|^3}4\pi G^2 M \ln\Lambda \int_0^{V_m} f_{_D} 4\pi v^2 dv\,, \quad (11)$$

where we have set $(M+m)\approx M$, and estimate the Coulomb logarithm as $\ln\Lambda = 4$; also here V_m is the smaller of V and $[2\xi(r)]^{1/2}$, the latter being the escape velocity from the system. Defining $x_m^2 = V_m^2/2\sigma_{_D}^2$, we get

$$\frac{d\vec{V}}{dt} = -\frac{\vec{V}}{V^3}4\pi G^2 M\rho_{_D}\ln\Lambda \times\left[e^{y_D}\left\{\mathrm{erf}(x_m) - \frac{2x_m}{\sqrt{\pi}}e^{-x_m^2}\right\} - \frac{4}{3\sqrt{\pi}}x_m^3\right]. \quad (12)$$

Thus, we have at hand the formalism needed to fit the observed profiles of number counts and of dispersion in the stellar velocity and obtain the parameters $\rho_D(0)$ and σ_D crucial to the phase-space distribution function of the dark matter particles. These will allow us to use Equation (12) to evaluate the dynamical friction effects on the globular clusters in Fornax.

3. COMPARISON WITH OBSERVATIONS

The theoretical profiles $v_{\rm rms*}(R)$ and $\Sigma_*(R)$ depend on the choice of the model parameters: ρ_{CD} (or more conveniently $\rho_D(0)$), σ_D, r_{KD} for the dark matter and ρ_{C*} (or $\rho_*(0)$), σ_* and r_{K*} for the stars. Amongst these $\rho_*(0)$ provides the normalization constant for $\Sigma_*(R)$ for the particular type of stars which are being counted, and r_{K*} the location where we would like to cut-off the stellar distribution. Noting that the farthest data point in the stellar profile observed by Coleman et al. (2005) lies at a projected distance $R\approx 4$ kpc, we may choose r_{K*} to be any value significantly greater than this, say 10 kpc. The observed profile is insensitive to this choice. Similarly the dependence of r_{KD} is also weak, fixing the total mass of the dark matter halo. Thus the crucial parameters that control the theoretical predictions are σ_*, σ_D and $\rho_D(0)$. It may be appropriate to point out here that $y_D(0)$ and $y_*(0)$ are not additional independent parameters. The choice of $\rho_D(0)$, σ_D, r_{KD} and corresponding stellar parameters fixes them through the requirement that $y_D(r_{KD}) = 0$ and $y_*(r_{K*}) = 0$.

We start by fitting the observed luminosity profile $\Sigma_*(R)$ based on the embedding model presented in the earlier sections. Our fit is shown in Figure 1 for the following set of parameters:

$$\rho_D(0) = 0.04\ M_\odot\ \mathrm{pc}^{-3},\ \sigma_D = 19.5\ \mathrm{km\ s}^{-1},\ \sigma_* = 12\ \mathrm{km\ s}^{-1}. \quad (13)$$

Note that the model fits the observations very well, including the power law tail at large radii. In contrast, a single-component King model does not fit the observations, as noted by Coleman et al. (2005). We emphasize that the fit to $\Sigma_*(R)$ is very sensitive to the choice of $\rho_D(0)$, σ_D, and σ_*, and at most a ten percent variation may be accommodated in the values of these parameters given in Equation (13). The values of $\rho_{_D}(0)$ and σ_* determine approximately the core radius of the stellar distribution in the embedding model; this radius, $r_{0*} = [9\sigma_*^2/4\pi G\rho_D(0)]^{1/2} = 650$ pc, marks the location where the projected stellar density falls to about one half of its central value. It is worth noting here that the quantity $\left(2\sigma_{_D}^2/\sigma_*^2\right)$ yields approximately $d\ln\rho_*(r)/d\ln(r)$, i.e. the power law exponent of the fall off of $\rho_*(r)$ beyond the core; or equivalently, $\left[\left(2\sigma_{_D}^2/\sigma_*^2\right)-1\right]$ gives the index for $\Sigma_*(R)$.

In order to ensure that our model is consistent with all the rest of the available observations, we calculate $\langle v_{r*}^2(R)\rangle^{1/2}$ with the same set of parameters fixed by fitting $\Sigma_*(R)$, and compare the prediction with the observed radial velocity dispersion (Walker et al. 2006). The data and our fit are shown in Figure 2. Even though the statistical uncertainties in the data set are large, our model is consistent with the observations. On the other hand, as pointed out by Walker et al., their observations are inconsistent with the single component King model (dashed line).

Having fixed the parameters of the model, it is a straightforward matter to calculate dynamical friction effects on the globular clusters using Equation (12). A convenient way to display the results is to assume circular orbits at various radial distances of closest approach and calculate the dynamical friction rate for $V = v_c$, where v_c is the circular velocity. There are two reasons for doing so: (1) if dynamical friction effects were indeed significant, then the orbits of the globular clusters would tend to be circularized by friction; (2) dynamical friction effects are maximized in the circular case, because noncircular orbits with the same distance of closest approach have higher velocities, and they also sample the outer, low-density regions of the dark matter distribution.

Choosing the best-fit parameters, $\rho_D(0) = 0.04\ M_\odot\ \mathrm{pc}^{-3}$ and $\sigma_D = 19.5\ \mathrm{km\ s}^{-1}$, we calculate the rate of dynamical friction given in Equation (12) and plot it in Figure 3. Very close to the center (i.e., for small r) the dynamical friction formula (12) simplifies to

$$\frac{d\vec{V}}{dt} \approx -\frac{16\pi^2 G^2 M\ln\Lambda\rho_{_D}(0)}{3\left(2\pi\sigma_{_D}^2\right)^{3/2}}\vec{V}\,, \quad (14)$$

which implies a lifetime

$$\tau \approx \left|\frac{V}{dV/dt}\right| = \frac{3\sigma_{_D}^3}{4\sqrt{2\pi}G^2 M\ln\Lambda\rho_{_D}(0)} \approx 4.5\ \mathrm{Gyr} \quad (15)$$

for globular clusters in Fornax. This simple estimate is consistent with the exact calculations presented in Figure 3. The effective lifetime, τ, is ~ 4.5 Gyr in the central parts of the dwarf spheroidal galaxy, it is nearly constant out to the core radius, and for larger radii it increases roughly quadratically with R. Since it would take several e-folding times for a globular cluster to sink to the center, even a globular cluster initially formed in the core region would not have migrated to the center within a Hubble time. For globular clusters that condensed in the outer regions or with elongated orbits, the effects of dynamical friction are much weaker than this estimate.

To be more specific, the dynamical friction causes loss of angular momentum at a rate

$$\frac{dL}{dt} = r\frac{dv}{dt}\,. \quad (16)$$

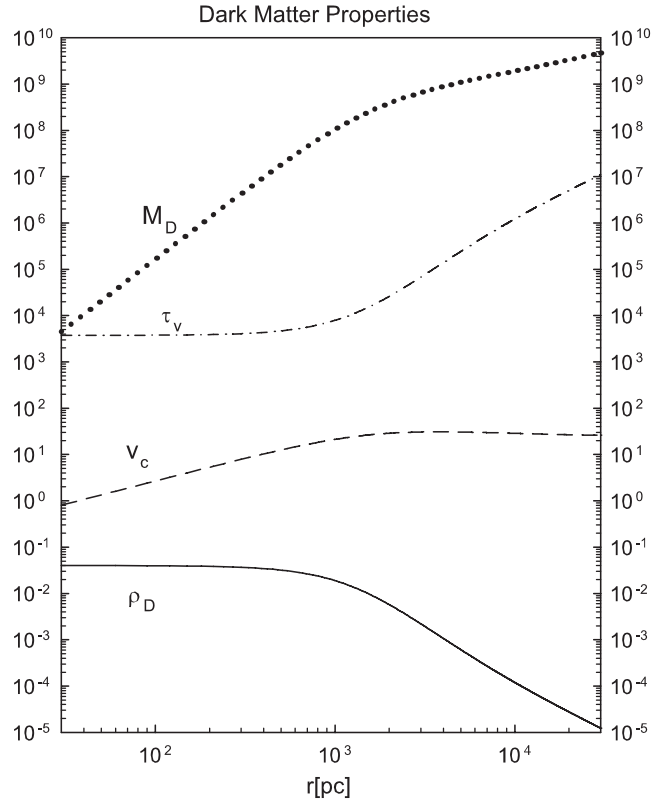

Figure 3. Lifetime $\tau_v = |V/(dV/dt)|$ for orbital decay due to dynamical friction, in Myr (dash-dotted line) is calculated for circular orbits, using the best-fit parameters for the dark matter distribution obtained from the observed stellar velocity dispersion and stellar density profiles. For completeness, we also show the enclosed mass in dark matter M_D in units of $M_\odot$ (dotted line), the circular speed v_c in km s^{-1} (dashed line), and the density of dark matter ρ_D in $M_\odot$/pc^3 (solid line).

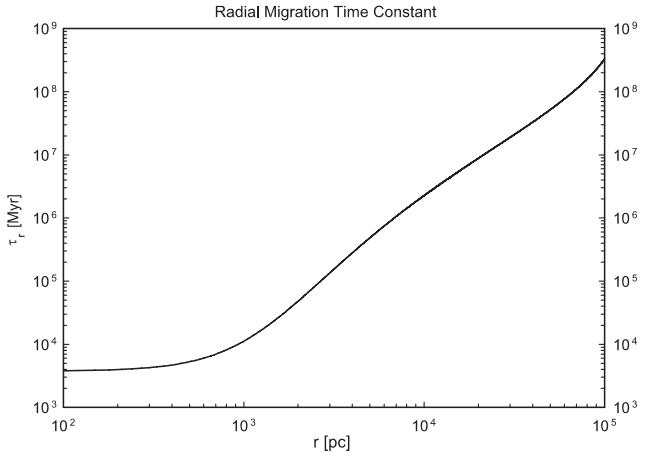

Figure 4. Radial migration time constant $\tau_r = r/|dv/dt|$ is displayed as a function of r.

Here the angular momentum L is taken to be $r \cdot v_c$, and the dynamical friction dv/dt is evaluated using Equation (12) with $V = v_c$, keeping in mind that friction will tend to make the orbits circular. For a given perigalacticon circular orbits suffer the highest rate of dynamical friction, as elliptical orbits will spend a large part of their orbital time in the lower density outer regions. In order to calculate the radial migration rate, we write

$$\frac{dr}{dt} = \left(\frac{dL}{dt}\right) \Big/ \left(\frac{dL}{dr}\right) = \left(r\frac{dv}{dt}\right) \Big/ \frac{d}{dr}(r \cdot v_c) \qquad (17)$$

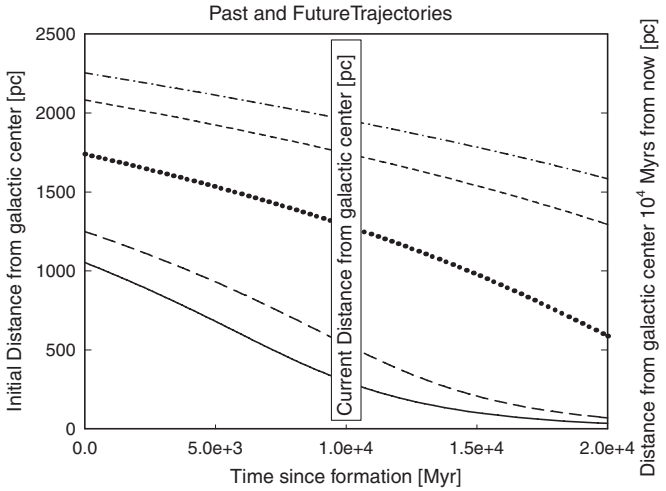

Figure 5. Radial trajectories of globular clusters from the time of the formation up to 10 Gyr in the future is shown. The trajectories pass through their present location, $r = \sqrt{3/2}R$, 10 Gyr after formation.

and define the radial migration time constant τ_r by

$$\tau_r(r) \approx r \Big/ \left|\frac{dr}{dt}\right| . \qquad (18)$$

This quantity is plotted in Figure 4. Note that τ_r becomes very large in the outer region, and becomes equal to τ_v well within the core radius. Indeed, the radial migration rate given in Equation (17) is easily integrated to obtain $r(t)$ for various assumed values of r_n, the present location of the globular clusters in Fornax. We show in Figure 5 the past and the future trajectories, starting from the time of their formation $\sim 10^4$ million years ago, arriving at their current location in the present epoch, and moving into the future another 10^4 million years. These trajectories exclude any paradoxical behavior and are consistent with the astrophysical assessment of the regions of their formation and subsequent evolution of their orbits. They show that the globular clusters that were formed at distances between $\sim$1 and 2 kpc from the center of Fornax, suffered dynamical friction at the expected rate and arrived at their current locations at the present epoch. During the next 10 billion years they will migrate closer to the center, but will remain distinct without forming a nucleus.

Thus the apparent paradox posed by the diffuse distribution of globular clusters in the Fornax dwarf spheroidal galaxy (Oh et al. 2000) is resolved. In order to provide some of the derived parameters of the stellar component in Fornax, we take the total visible magnitude of Fornax $m_L \approx 9.3$ (Karachentsev et al. 2004), distance $d = 138$ kpc and a bolometric correction $\sim 1^m$ to estimate the total luminosity of $L \approx 7.5 \times 10^6\ L_\odot$. (For a bolometric correction of $\sim 0.5^m$, $L \approx 6 \times 10^6\ L_\odot$). In Figure 6 we show the density of the stars $\rho_*(r)$ in arbitrary units, the luminosity within a radius r and the mass-to-luminosity ratio as a function of the radius; of course the mass is dominated by the dark matter.

4. DISCUSSION AND CONCLUSIONS

The dynamical friction suffered by astronomical objects (such as globular clusters) depends not only on the local spatial density of the surrounding region, but also on its phase-space structure. Since the phase-space density is invariant along a dynamical

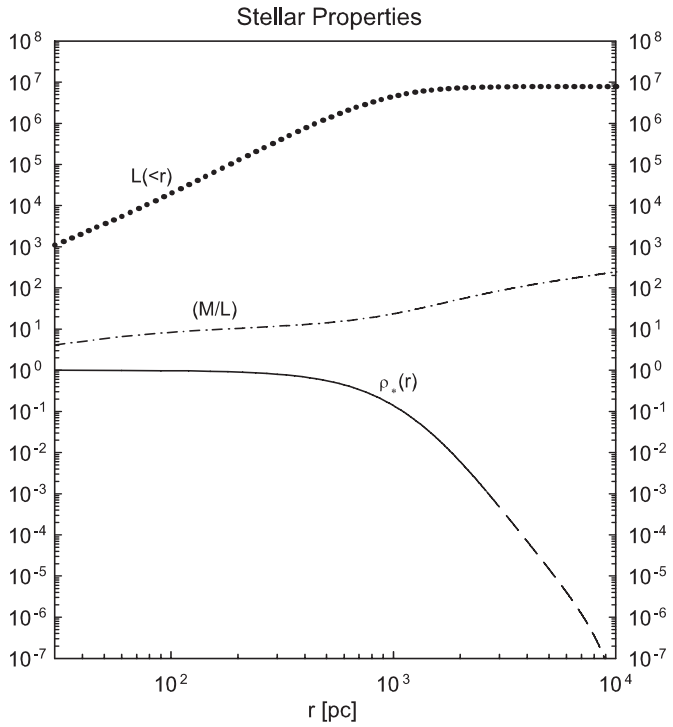

Figure 6. Theoretical estimates of the stellar density $\rho_*(r)$ in $M_\odot/\mathrm{pc}^3$ (solid line), stellar luminosity L enclosed within a radius r in $L_\odot$ (dotted line) and the total mass-to-luminosity ratio M/L also enclosed within r in units of $M_\odot/L_\odot$ (dash-dotted line) are shown as a function of the radial coordinate. Note that the density of stars becomes less than one thousandth of its central value for $r > 3$ kpc, and it is unclear whether these stars really belong to the dwarf galaxy. This is indicated by the dashed-line extension to the model estimates of $\rho_*(r)$.

trajectory, this sensitivity implies that several parameters of interest (such as the dispersion velocities and the extent of the dark matter halo) may be determined by examining the role played by dynamical friction in extended structures in the universe. These remarks are illustrated here through a study of the dynamics of globular clusters surrounding the dwarf spheroidal galaxy in Fornax. To summarize, a model based on reduced isothermal distributions both for the stars and the dark matter provides a very good fit to the radial velocity dispersions $v_{\mathrm{rms}*}(R)$ and the luminosity profile $\Sigma_*(R)$ observed for the stars in the dwarf spheroidal in Fornax. These fits determine $\rho_D(0)$ and σ_D, the two crucial parameters of the phase-space distribution of dark matter. The rates of dynamical friction calculated using these parameters are sufficiently small that the paradox pointed out by Oh et al. (2000) is resolved. An application of such models to other systems including galaxy clusters would provide further insight into the phase-space distribution of dark matter and the process of structure formation in the universe. The parameters derived in this paper add support to the correlations derived for dark matter halos by Kormendy & Freeman (2004). It would also be useful to attempt self-consistent fits to the observations of Fornax, using the phase-space distributions obtained with numerical simulations, as soon as they become available.

We thank Dr. Tsitsi Madziwa-Nussinov for help with the preparation of the manuscript, and Professor Francesc Ferrer for discussions.

REFERENCES

Aaronson, M. 1983, ApJ, 266, L11
Binney, J., & Tremaine, S. 2008, Galactic Dynamics (Princeton, NJ: Princeton Univ. Press)
Chandrasekhar, S. 1943, ApJ, 97, 255
Coleman, M., et al. 2005, AJ, 129, 1443
Cowsik, R., & Ghosh, P. 1986, JA&A, 7, 7
Cowsik, R., & Ghosh, P. 1987, ApJ, 317, 26
Ciotti, L., & Binney, J. 2004, MNRAS, 351, 285
Faber, S. M., & Lin, D. N. C. 1983, ApJ, 266, L17
Gilmore, G., et al. 2007, ApJ, 663, 948
Goerdt, T., et al. 2006, MNRAS, 368, 1073
Hernandez, X., & Gilmore, G. 1998, MNRAS, 297, 517
Hernquist, L. 1990, ApJ, 356, 359
Hodge, P. W. 1961a, ApJ, 66, 83
Hodge, P. W. 1961b, ApJ, 66, 249
Irwin, M., & Hatzidimitriou, D. 1995, MNRAS, 277, 1354
Karachentsev, I. D., Karachentseva, V. E., Hutchmeir, W. K., & Makarov, D. I. 2004, AJ, 127, 2031
King, I. R. 1966, AJ, 71, 64
Kormendy, J., & Freeman, K. C. 2004, in IAU Symp. 220, Dark Matter in Galaxies, ed. S. D. Ryder et al. (San Francisco, CA: ASP), 377
Levin, Y., Pakter, R., & Rizzato, F. B. 2008, Phys. Rev. E, 78, 021130 (references therein)
Lotz, J., et al. 2001, ApJ, 552, 572
Lynden Bell, D. 1967, MNRAS, 136, 101
Mateo, M. 1998, ARA&A, 36, 435
Moore, B., et al. 1999, ApJ, 524, 19
Navarro, J. F., Frenk, C. S., & White, S. D. M. 1997, ApJ, 490, 493
Oh, K. S., et al. 2000, ApJ, 531, 727
Pryor, C., & Kormendy, J. 1990, AJ, 100, 127
Sánchez-Salcedo, F. J., Reyes Iturbide, J., & Hernandez, X. 2006, MNRAS, 370, 1829
Tremaine, S. 1976, ApJ, 203, 345
Walker, M., et al. 2006, AJ, 131, 2114